

# Scanning Electrochemical Microscopy. 23. Reaction Localization of Artificially Patterned and Tissue-Bound Enzymes

David T. Pierce<sup>†</sup> and Allen J. Bard\*

Department of Chemistry and Biochemistry, The University of Texas at Austin, Austin, Texas 78712

**The scanning electrochemical microscope (SECM), operating in the feedback mode, was used to image localized surface reactions of redox enzymes at the micrometer level. Surfaces imaged with the SECM included glucose oxidase immobilized within 8-μm-diameter pores of a filtration membrane and individual whole mitochondria with active NADH cytochrome reductase enzymes in their outer membranes. Factors influencing enzyme image resolution and specificity are discussed.**

## INTRODUCTION

Methods for detection, characterization, and localization of enzymes within specific tissues have received considerable attention.<sup>1–3</sup> In much of this work, tissue fractionation methods and conventional (optical) microscopic techniques play complimentary roles because neither method alone can adequately satisfy each analytical function. With the former methodology, cell structures suspected of enzymatic activity are isolated from a tissue homogenate and then analyzed using standard assay techniques.<sup>4</sup> With these procedures, enzyme content can usually be quantified with high precision and kinetic behavior can be assessed reliably. However, these methods do not provide information about an enzyme's location on or within the isolated cell structure or about the possible contamination of the isolate with materials from other enzyme-bearing structures. Microscopic methods suffer less from these deficiencies, since an effort is made to keep the enzyme-containing tissues intact and thus preserve the reaction site morphology. In most microscopic studies, chemical procedures are first used to fix the tissue and then to stain or mark the reaction sites of the target enzyme. The samples are then observed, in most cases, using transmission electron or optical microscopies<sup>5</sup> or by a variety of microfluorometric methods.<sup>6</sup> Although these microscopic techniques can achieve micrometer to submicrometer resolution and can determine enzyme location in even subcellular structures, they usually do not quantify or kinetically characterize the reactions catalyzed by the target enzyme.

As a potential method for simultaneous *in situ* analysis of enzyme function and location, the scanning electrochemical microscope (SECM)<sup>7</sup> has been applied recently to the study

of a variety of biocatalytic surface reactions. Wang et al. studied the surface reactions of immobilized enzymes and enzyme-containing tissues by the collection electrolysis of enzymatically generated compounds at a microelectrode.<sup>8</sup> Imaging of enzyme location was also attempted in this work by using the same electrolysis scheme. However, the effective lateral resolution of these images (200–250 μm<sup>2</sup> per point) was well below that of the SECM. Although qualitative, these results demonstrated that enzyme surface reactions could be detected using the SECM and that the scanning ability of the SECM could be used to map reactive sites. Recently, we demonstrated that steady-state surface reactions involving redox-active enzymes (oxidoreductases) can be quantitatively studied with the SECM using a feedback electrolysis scheme.<sup>9</sup> This feedback method of detection, which differs significantly from the earlier applied collection methodology, is illustrated in Figure 1 and provides several advantages for quantifying and imaging surface reactions.

In collection experiments, a substrate specific to the enzyme reaction ( $S_1$ ) is present in the assay solution, and the catalyzed reaction occurs continuously over the entire surface in areas occupied by the enzyme (Figure 1a). The production of enzyme-generated product begins when the reactants are added to the cell so that a concentration profile forms around the enzyme site that extends into the solution. In most cases, there is no way to switch the enzyme reaction on and off. In feedback experiments, the enzyme reaction only occurs in close proximity to the SECM probe tip where an enzyme substrate,  $S_1$ , is electrochemically generated (Figure 1b). Here, the SECM tip is used to initiate and sustain the enzyme reaction because it provides the only source of substrate. For modeling purposes and quantitation of surface reaction kinetics, the feedback approach is better than the collection approach, because the current monitored at the probe tip gives a well-defined measure of the amount of substrate being produced at the tip (equivalent to the amount of substrate available to the enzyme) and the amount of product fed back to the tip (equivalent to the amount of substrate consumed by the enzyme). For imaging purposes, the feedback methodology also provides better lateral resolution because the enzyme reaction product ( $P_1$ ) diffuses only a short distance before it is detected by the tip. In the collection mode, product is generated continuously over the entire enzyme surface. This situation can lead to the overlap of product diffusion zones from different individual enzyme sites. Such diffusional overlap can perturb kinetic measurements when the product diffuses into regions where no enzyme reaction is actually occurring and can seriously blur the SECM image and degrade resolution.<sup>10</sup>

The SECM appears to be a promising technique for *in situ* enzyme analysis because of its ability to gather detailed kinetic and mechanistic information relevant to enzyme function

\* Present address: Department of Chemistry, University of North Dakota, Grand Forks, ND 58202.

(1) *Methods in Enzymology*; Academic: New York, 1955ff.

(2) *Methods of Enzymatic Analysis*, 3rd ed.; Bergmeyer, H. U., Ed.-in-chief; Bergmeyer, J., Grassl, M., Eds.; VCH Publishers: Weinheim, Germany, 1986; Vol. 1–12.

(3) *The Enzymes*; Boyer, P. D., Ed.; Academic: New York, 1970ff.

(4) *Enzyme Analysis. A Practical Approach*; Eisenthal, E., Danson, M. J., Eds.; Oxford University Press: Oxford, U.K., 1992.

(5) *Electron Microscopy of Enzymes: Principles and Methods*; Hayat, M. A., Ed.; Van Nostrand Reinhold: New York, 1973; Vol. 1–5.

(6) Sernetz, M.; Puchinger, H. In *Methods in Enzymology*; Mosbach, K., Ed.; Academic: New York, 1976; Vol. 44, p 373.

(7) Bard, A. J.; Fan, F.-R. F.; Pierce, D. T.; Unwin, P. R.; Wipf, D. O.; Zhou, F. *Science* 1991, 254, 68, and references therein.

(8) Wang, J.; Wu, L.-H.; Li, R. *J. Electroanal. Chem. Interfacial Electrochem.* 1989, 272, 285.

(9) Pierce, D. T.; Unwin, P. R.; Bard, A. J. *Anal. Chem.* 1992, 64, 1795.

(10) Lee, C.; Wipf, D. O.; Bard, A. J.; Bartels, K.; Bovik, A. C. *Anal. Chem.* 1991, 63, 2442.

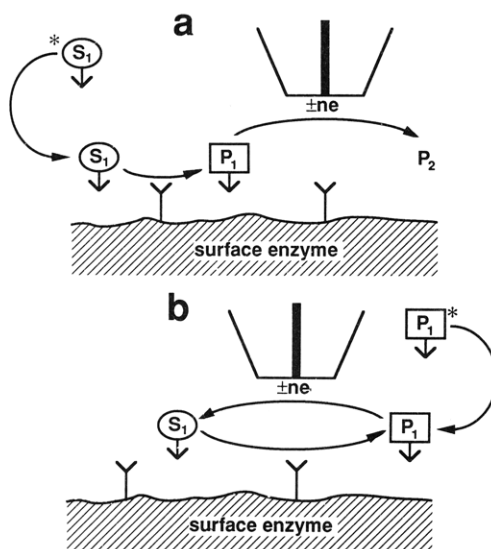


**Figure 1.** Schematics depicting the principles of SECM: (a) collection-mode and (b) feedback-mode detection of redox-active enzyme substrates ( $S_1$ ) and products ( $P_1$ ). Species present in bulk solution are identified with asterisks. For example, in the feedback mode with glucose oxidase (GO), hydroquinone ( $P_1$ ) in solution reacts at the tip to form quinone ( $S_1$ ), which reacts at the enzyme (GO) site with D-glucose to produce hydroquinone.

and its capacity to study this function with enzymes in their native environment, namely, localized on or within membranes and perfused with buffered electrolyte. In this paper, we extend our earlier work with the feedback detection of redox enzymes<sup>9</sup> and demonstrate the SECM's ability to resolve spatially sites or tissues where specific enzyme reactions occur. We also discuss the experimental factors that determine the SECM's enzyme specificity as well as its ultimate resolution for enzyme localization.

## EXPERIMENTAL SECTION

**Materials.** All chemicals were obtained from commercial sources and were used without further purification unless otherwise noted.  $\alpha$ -D-Glucose (ACS reagent), hydroquinone ( $H_2Q$ ; +99%) methyl viologen dichloride ( $MVCl_2$ ; 98%), and *N,N,N',N'*-tetramethyl-p-phenylenediamine (TMFD; 98%) were obtained from Aldrich Chemical Co. Solutions containing  $\alpha$ -D-glucose, used as a precursor to the enzyme-specific reactant  $\beta$ -D-glucose, were prepared at least 24 h before each experiment at room temperature to allow complete equilibration of the  $\alpha$ - and  $\beta$ -anomers. TMFD was sublimed twice under vacuum and stored under nitrogen before use. Bovine serum albumin (BSA; 98–99%) and glucose oxidase (GO, EC 1.1.3.4; type X from *Aspergillus niger*, 125 IU  $mg^{-1}$  (35 °C), 186 000 g  $mol^{-1}$ ) were obtained from Sigma Chemical Co., as were  $\beta$ -nicotinamide adenine dinucleotide (reduced disodium salt,  $\beta$ -NADH; No. N 8129), sodium azide, rotenone (95–98%), and antimycin A. Ultrapure sucrose (99.9%) was obtained from ICN Biochemicals. Poly(ethylene glycol) diglycidyl ether (PEG 400) was obtained from Polysciences, Inc. Solutions used in all experiments were prepared with 18 MΩ cm Milli-Q reagent water (Millipore Co.).

Whole liver mitochondria were isolated as a suspension from male Sprague-Dawley albino rats in 0.25 M sucrose by the procedure of Johnson and Lardy.<sup>11</sup> Mitochondria suspensions were stored at 5 °C and used within 1–2 days. Protein determinations of mitochondrial extracts were made by the standard biuret method.

**Electrochemical Procedures.** In voltammetric experiments, a small-volume glass cell (0.2–1.0 mL) was employed; this contained a Pt auxiliary electrode, a Ag quasi-reference electrode (AgQRE), a glassy carbon disk electrode (Bioanalytical Systems (BAS), West Lafayette, IN, 1.57-mm radius), and a port for argon

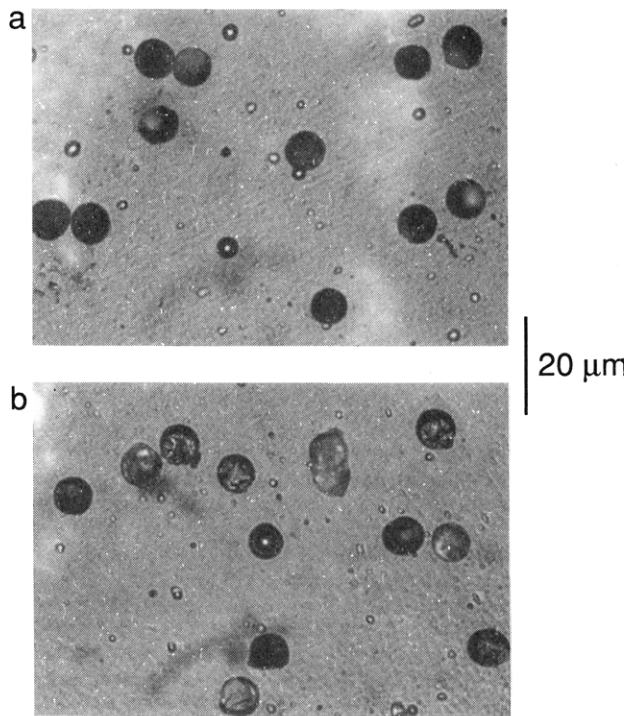


**Figure 2.** Optical microscope photographs of filtration membrane surfaces. Average pore diameter is 8–10  $\mu m$ . (a) Untreated membrane surface. (b) Membrane surface treated with glucose oxidase hydrogel.

blanketing. Measurements were carried out with a BAS 100B electrochemical analyzer.

A two-electrode Teflon cell (1–2 mL) described previously<sup>9</sup> was used in all SECM experiments. The working ultramicroelectrode used in all cases was a carbon fiber (electrode radius  $a = 4.0 \pm 0.5 \mu m$ ) sealed in Pyrex that was polished to a radius  $10 \pm 2$  times the fiber radius at the exposed tip (i.e., ratio of glass sheath radius to electrode radius  $RG = 10$ ). The tip was polished with 0.05- $\mu m$  alumina before each experiment. The scanning electrochemical microscope and operating procedures used for imaging were similar to those described previously.<sup>12</sup>

Experimental conditions specific to the monitored enzyme reactions are given with individual results. All experiments were performed at ambient temperature (22–25 °C).

**Patterning of GO.** Relatively flat surfaces containing well-defined areas of glucose oxidase were fabricated by immobilizing a GO hydrogel within the track-etched pores of polycarbonate filtration membranes (Nuclepore Co.). The hydrogel matrix containing GO, similar to that developed by Heller and co-workers,<sup>13,14</sup> has been described elsewhere.<sup>9</sup> Membranes with cylindrical pores 8–10  $\mu m$  in diameter were affixed to 1 × 1  $cm^2$  glass slides using double-sided tape. Aqueous 20 wt % solutions of BSA, GO, and PEG 400 were combined thoroughly in a volume ratio of 20:25:5, respectively, and the mixture was distributed evenly over the membrane surface. Coated membranes were cured at 35 °C for 48 h, allowing the hydrogel to harden within the membrane pores and as a thin, cracked layer on the membrane surface. After full curing, the surface layer was gently brushed away. Optical microscope color photographs taken before addition of GO and after removal of the surface layer indicated that the yellow hydrogel was immobilized within 80–90% of the membrane pores. Black-and-white reproductions of these photographs (Figure 2) only show the hydrogel as bright corrugations within a majority of pores. These bright corrugations (Figure 2b) were absent in untreated membranes (Figure 2a).

**Immobilization of Mitochondria.** For each sample prepared, a 50- $\mu L$  aliquot of freshly isolated mitochondria was added to 50  $\mu L$  of 5% glutaraldehyde in 0.25 M sucrose that was already distributed over a 1 × 1  $cm^2$  aminated<sup>10</sup> glass slide. The solutions were thoroughly mixed, and after standing 5 min, each slide was

(12) Wipf, D. O.; Bard, A. J. *J. Electrochem. Soc.* 1991, 138, 469.

(13) Gregg, B. A.; Heller, A. *J. Phys. Chem.* 1991, 95, 5976.

(14) Pishko, M. V.; Michael, A. C.; Heller, A. *Anal. Chem.* 1991, 63, 2268.

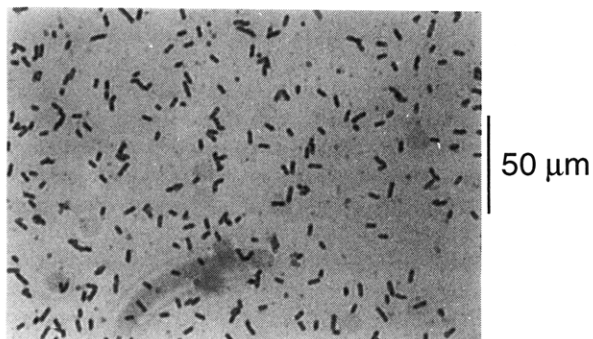


**Figure 3.** Optical microscope photograph of glass-immobilized rat liver mitochondria.

gently rinsed with 0.25 M sucrose and stored in a buffer electrolyte (0.1 M KCl, 0.25 M sucrose, 50 mM phosphate buffer, pH 7.5) at 5 °C. Optical photographs of identically prepared slides showed a wide variation in the number and distribution of immobilized mitochondria (0–20 mitochondria per 50 × 50 μm square) and also indicated some clumping (Figure 3).

## RESULTS AND DISCUSSION

**SECM Imaging of GO Catalysis.** The first step toward spatially resolving the surface reactions of glucose oxidase (GO) was to immobilize GO at small, well-defined sites on an insulating material. A variety of photolithographic methods have been used to bind GO in patterned surface regions.<sup>15</sup> However, these procedures are time-consuming and typically yield poor spatial resolution of the enzyme (areas >50 μm<sup>2</sup>). Recently, methods for trapping GO within preexisting surface structures have demonstrated better surface localization (areas <1 μm<sup>2</sup>) with easier preparation.<sup>16</sup> Using track-etched filtration membranes as prepatterned surfaces, we employed a similar trapping scheme (see Experimental Section) in this work to localize GO hydrogel within membrane pores. These treated membranes were adequate to test the reaction imaging ability of the SECM.

The feedback electrolysis method used to image membrane sites of GO catalysis has been described in detail<sup>9</sup> and is illustrated in Figure 1b. Briefly, membrane surfaces containing local sites of GO hydrogel were bathed in a buffered assay solution containing the GO specific reductant β-D-glucose, as well as an electrochemically oxidizable mediator (P<sub>1</sub>). A microelectrode was then positioned in the solution at a distance a few electrode radii above the surface, and a potential was applied which oxidized the mediator to form an enzyme-reactive material (S<sub>1</sub>). If reduced GO was present within the diffusion field of the electrode, the mediator was reformed or fed back by reaction of S<sub>1</sub> with the enzyme. By maintaining D-glucose at a sufficiently high concentration to ensure that GO remained in its reduced state, usually 50 mM or higher, the current caused by the electrode reaction of P<sub>1</sub> was increased by an amount that was directly related to the concentration of active enzyme on the surface and the saturation kinetics of the glucose–GO reaction.

As a control, membrane samples impregnated with GO hydrogel were first imaged with the SECM under conditions where no enzyme reaction occurred with the mediator. Under these negative feedback conditions, the surface topography around the membrane pores could be determined. Elimination of enzyme feedback was typically accomplished by using assay solutions without D-glucose or by using a reducible redox mediator. Figure 4 shows a negative feedback image collected with an 8-μm-diameter carbon fiber microelectrode

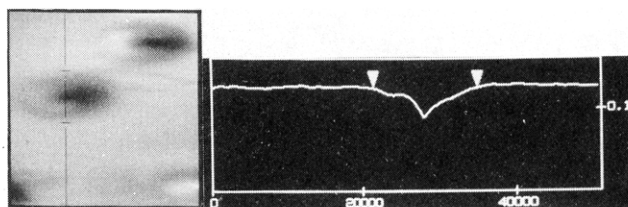


**Figure 4.** SECM image (50 × 50 μm) with line section of a GO hydrogel-treated membrane surface. Image was taken with a carbon microelectrode tip ( $a = 4.0 \mu\text{m}$ ,  $\text{RG} = 10$ ,  $\text{rate} = 10 \mu\text{m s}^{-1}$ ) at +0.82 V vs AgQRE in 0.1 M phosphate-perchlorate buffer (pH 7.0) containing no D-glucose, 50 μM H<sub>2</sub>Q, and 100 μM MVCl<sub>2</sub>. Lightest image regions depict the greatest normalized tip currents ( $I/I_0$ ).

(glass radius of 10 × fiber radius,  $\text{RG} = 10$ ) and with a buffered assay solution containing the mediator and hydroquinone, but no D-glucose. The darkest regions (lowest currents) indicated high points on the membrane surface where fractured GO hydrogel protruded out of individual pores and blocked diffusion of the mediator to the electrode. Image cross sections through these high points, as shown in Figure 4, demonstrated that the width of each feature (12–14 μm) was slightly larger than the average pore diameter determined by optical microscopy (8–10 μm). These results indicated that some diffusional blurring of the image occurred because of the comparable sizes of the carbon fiber–glass insulator tip and the membrane pores. Some images showed very light regions (highest currents) that indicated low points with the same areas as the hydrogel protrusions (e.g., lower right in Figure 4). These features indicated a smaller number of the pores that were not filled with GO hydrogel near the surfaces. The negative feedback SECM images were generally consistent with optical photographs taken of identically treated membrane surfaces (Figure 2b).

A direct test of the SECM's ability to image GO catalysis over a localized surface region is shown in Figure 5. Both images were collected in sequential passes over the same hydrogel-filled pore and with exactly the same solution and scan parameters. The only difference between the images was the potential applied to the microelectrode tip. The buffered assay solution contained a high concentration of D-glucose as well as two SECM redox mediators, methyl viologen dication (MV<sup>2+</sup>) and neutral hydroquinone (H<sub>2</sub>Q). Figure 5a shows an image obtained with a tip potential of −0.95 V vs AgQRE where methyl viologen dication was reduced to the monocation species (MV<sup>•+</sup>). Since MV<sup>•+</sup> does not react with reduced GO on the hydrogel protrusion, a negative deflection in the current, similar to Figure 4, was obtained. However, with the tip potential changed to +0.82 V vs AgQRE, where hydroquinone was oxidized to the p-benzoquinone species, the image in Figure 5a clearly demonstrated an increased current over the same pore. Since p-benzoquinone is readily reduced back to hydroquinone by reduced GO, this positive deflection over the hydrogel protrusion indicated a large catalytic feedback of the hydroquinone mediator and provided a direct image of the local enzyme reaction.

**Mitochondrion-Bound Enzyme.** To test the feasibility of SECM detection and localization on enzyme systems in actual organelles, rat liver mitochondria were chosen as samples because of their relatively small size (3–5 μm in diameter) and diverse composition of redox-active enzymes.<sup>17</sup> The particular mitochondrial enzyme studied here is the NADH–cytochrome c reductase system (EC 1.6.99.3).<sup>18</sup> These enzymes reside on the outer membrane of rat liver mitochondria<sup>19</sup> and are highly active in their bound and solubilized forms. For example, one of the integral units in this system

(15) Vopel, T.; Ladde, A.; Hüller, H. *Anal. Chim. Acta* 1991, 251, 117, and references therein.

(16) Koopal, C. G.; de Ruiter, B.; Nolte, R. J. M. *J. Chem. Soc., Chem. Commun.* 1991, 1691.

(17) *Textbook of Biochemistry: With Clinical Correlations*, 3rd ed.; Devlin, T. M., Ed.; Wiley-Liss: New York, 1992.

(18) *Enzyme Handbook*; Barman, T. E., Ed.; Springer-Verlag: New York, 1969; Vol. 1.

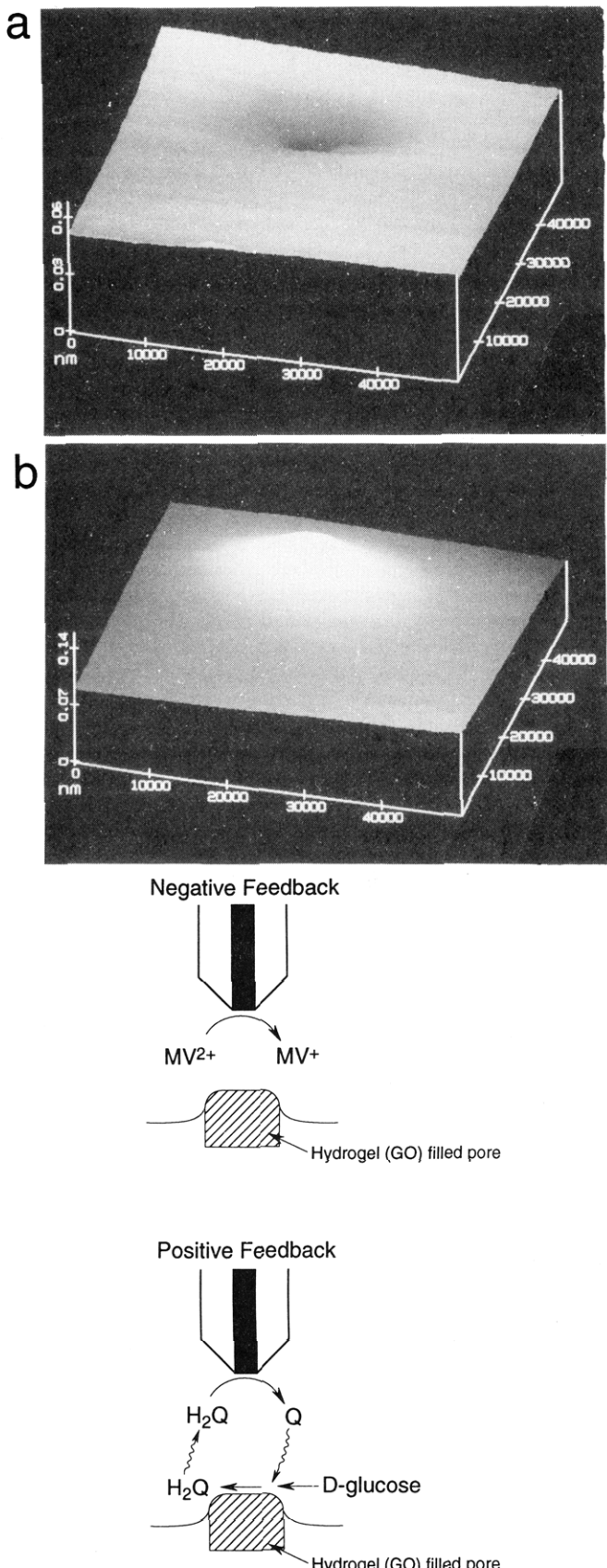


**Figure 5.** SECM surface-plot images ( $50 \times 50 \mu\text{m}$ ) of a single GO hydrogel-filled pore on the surface of a treated membrane and schematic representations of SECM conditions. Images were taken with a carbon microelectrode tip ( $a = 4.0 \mu\text{m}$ ,  $RG = 10$ , rate =  $10 \mu\text{m s}^{-1}$ ). (a) Negative feedback with  $MV^{2+}$  mediator at tip potential  $-0.95 \text{ V vs AgQRE}$ . (b) Positive feedback with hydroquinone ( $H_2Q$ ) mediator at tip potential  $+0.82 \text{ V vs AgQRE}$  in  $0.1 \text{ M}$  phosphate-perchlorate buffer ( $pH = 7.0$ ) containing  $100 \mu\text{M D-glucose}$ ,  $50 \mu\text{M H}_2Q$ , and  $100 \mu\text{M MVCl}_2$ . Lightest image regions depict the greatest normalized tip currents ( $i/i_{t,\infty}$ ).

is the flavoprotein NADH-cytochrome  $b_5$  reductase (EC 1.6.2.a).<sup>18</sup> This protein exhibits a maximal solubilized turnover of  $29\,000 \text{ mol of substrate min}^{-1}$  (mol of reductase) $^{-1}$  at  $25^\circ\text{C}$ .<sup>20</sup> Since this turnover number was actually larger than the turnover assayed for the glucose oxidase used in this work ( $23\,000 \text{ mol of substrate min}^{-1}$  (mole of GO) $^{-1}$  at  $35^\circ\text{C}$ ), we felt the reductase catalysis should be detectable by the same feedback method applied in our SECM analysis of GO.

NADH-linked reductases catalyzed the reduction of an electron acceptor by NADH in an optimal pH range of  $5.5$ – $8.2$ . In this process, the enzyme receives two electrons from NADH in a single step and transfers these electrons to the acceptor (oxidant) in two one-electron steps.<sup>20</sup> In addition to its high turnover, a key feature of these enzymes from the standpoint of SECM analysis is their ability to be oxidized by many different acceptors and their high specificity for the reducing substrate (NADH). Several studies have shown that a number of oxidants could be substituted for the natural acceptors for NADH-linked reductases with little or no degradation in turnover rate. These oxidants include ferricyanide, ferricytochrome  $c$ , and oxidized  $N,N,N',N'$ -tetramethyl- $p$ -phenylenediamine (TMPD $^+$ ).<sup>19,21</sup> However, molecular oxygen only showed  $0.01\%$  of the maximum turnover rate when it acted as the acceptor.<sup>20</sup> The high specificity for the reductant,  $\beta$ -nicotinamide adenine dinucleotide (NADH), appears to be related to the dinucleotide structure and to the  $4\text{A}$ -hydrogen portions of the molecule.<sup>19,20</sup> For this reason, reductive substrates like NADPH and  $\alpha$ -NADH show little activity.

**Electrochemical Characterization of Mitochondrion Enzyme System.** Before initiating an SECM study of mitochondrion-bound NADH reductases, it was first necessary to determine whether the catalysis could indeed be driven rapidly and selectively in whole mitochondria by electrochemical methods. Hill and Sanghera<sup>22</sup> have established the use of cyclic voltammetry at conventionally sized electrodes (1–10-mm diameter) to test this type of electrocatalytic mediation with solubilized enzymes. We thus adopted this approach for testing and characterizing enzyme systems in whole mitochondria. Our results show that it is possible to detect and identify active mitochondrion-bound enzymes with cyclic voltammetry and to measure their maximal turnover rates in the presence of active and inhibitory substrates.

The electrochemical behavior of the mediator and substrate were initially observed by cyclic voltammetry in the absence of mitochondria to determine individual reactivity and redox compatibility. For the targeted NADH-cytochrome  $c$  reductase system, the mediator was TMPD and the substrate was NADH. The assay electrolyte in all cases was a  $50 \text{ mM}$  phosphate buffer ( $pH = 7.5$ ) containing  $0.1 \text{ M}$  KCl and  $0.25 \text{ M}$  sucrose. In this medium,  $0.5 \text{ mM}$  TMPD showed a diffusion-controlled, one-electron, chemically reversible oxidation centered at  $E_{1/2} = +0.021 \text{ V vs SCE}$  ( $+0.21 \text{ V vs AgQRE}$ ) and a second chemically irreversible oxidation wave at  $E_{p,a} = +0.463 \text{ V vs SCE}$  ( $100 \text{ mV s}^{-1}$ ). In a separate solution,  $0.5 \text{ mM}$  NADH showed a chemically irreversible oxidation at  $E_{p,a} = +0.479 \text{ V vs SCE}$  ( $100 \text{ mV s}^{-1}$ ). When TMPD and NADH were combined in equimolar amounts in the assay electrolyte, the first oxidation wave for TMPD remained unchanged (Figure 6a). However, at very high NADH concentrations,  $[NADH]/[TMPD] > 50$ , NADH was capable of directly reducing TMPD $^+$  formed at the electrode. This

(19) Sottocassa, G. L.; Kuylestierna, B.; Ernster, L.; Berstrand, A. *J. Cell Biol.* 1967, 32, 415.

(20) Mathews, F. S.; Czerwinski, E. W. In *Enzymes of Biological Membranes*; Plenum: New York, 1985; Vol. 4, pp 274–283.

(21) Bernardi, P.; Azzone, G. F. *Biochim. Biophys. Acta* 1982, 679, 19.

(22) Hill, H. A. O.; Sanghera, G. S. In *Biosensors: A Practical Approach*; Cass, A. E. G., Ed.; Oxford University Press: Oxford, U.K., 1990; pp 19–46, and references therein.

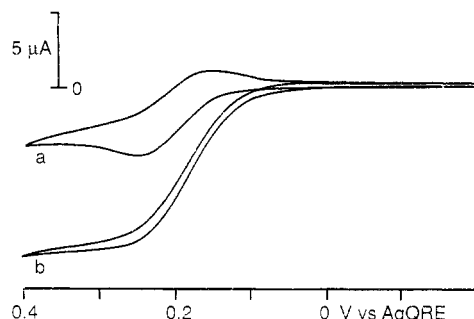


**Figure 6.** Cyclic voltammograms ( $10 \text{ mV s}^{-1}$ ) recorded at a glassy carbon disk electrode in separate  $50 \text{ mM}$  phosphate buffer solutions ( $\text{pH } 7.5$ ) containing  $0.1 \text{ M}$  KCl,  $0.25 \text{ M}$  sucrose,  $0.5 \text{ mM}$  TMPD, and (a)  $0.5 \text{ mM}$  NADH or (b)  $50 \text{ mM}$  NADH + whole rat liver mitochondria ( $35 \text{ mg of protein mL}^{-1}$ ).

reaction resulted in regeneration of  $\text{TMPD}^0$  that could be observed as sigmoidal distortions in voltammograms recorded at sweep rates below  $50 \text{ mV s}^{-1}$ . The working curves of Nicholson and Shain for EC' reactions<sup>23</sup> yielded a second-order rate constant of  $2.2 \pm 0.2 \text{ M}^{-1} \text{ s}^{-1}$  for this direct regeneration.

In assay electrolyte containing the combined substrates,  $[\text{NADH}] = 50 \text{ mM}$  and  $[\text{TMPD}] = 0.5 \text{ mM}$ , and suspended whole rat liver mitochondria ( $35 \text{ mg of protein per milliliter}$  of assay solution), voltammograms demonstrated larger sigmoidal curves (Figure 6b); these were observable even at scan rates up to  $1 \text{ V s}^{-1}$ . (To assure maximal activity of the NADH-cytochrome c reductase system, concentrations of TMPD and NADH were selected that were greater than  $10\times$  their apparent  $K_M$  values:  $K_{M,\text{TMPD}} = 19 \mu\text{M}$ ,<sup>21</sup>  $K_{M,\text{NADH}} = 100 \mu\text{M}$ .<sup>18</sup>) The current increase and sigmoidal shape was again indicative of  $\text{TMPD}^0$  regeneration at the electrode and was diagnostic of kinetic control of the electrode reaction. Applying the Nicholson and Shain EC' working curves<sup>23</sup> to the voltammetric data, a forward rate constant for catalyzed regeneration of  $k_{\text{cat}} = 2.0 \pm 0.1 \text{ s}^{-1}$  was calculated. Compared to the direct-regeneration pseudo-first-order forward rate constant of  $k_f = 0.12 \pm 0.05 \text{ s}^{-1}$  estimated under the same solution conditions, this 20-fold difference clearly indicated that the mitochondrial suspension actively promoted regeneration of neutral mediator,  $\text{TMPD}^0$ , at the electrode surface. The data also showed that the mitochondrial reaction could be driven electrochemically as long as the electrode provide a constant source of the oxidant (in this case,  $\text{TMPD}^+$ ).

Control experiments were also carried out to demonstrate which mitochondrial enzymes produced the enhanced regeneration rates. Initial control voltammograms were recorded in mitochondrial suspensions containing the acceptor substrate TMPD, but no NADH. These experiments showed only a purely diffusion-controlled wave for the  $\text{TMPD}^0/\text{TMPD}^+$  couple and no evidence of  $\text{TMPD}^0$  regeneration. Further control experiments were carried out in a mitochondrial suspension with both TMPD and NADH present, but with redox inhibitors to block internal mitochondrial electron transfer. Rotenone ( $0.5 \text{ mg mL}^{-1}$ ) was used to inhibit the flavoprotein, NADH dehydrogenase, antimycin A ( $0.3 \text{ mg mL}^{-1}$ ) was used to block electron transport at the level of cytochrome b, and sodium azide ( $3.5 \text{ mg mL}^{-1}$ ) was employed to block terminal electron transport to cytochrome oxidase.<sup>17</sup> Voltammetric curves recorded under these conditions showed nearly the same magnitude of  $\text{TMPD}^0$  regeneration as found in the absence of enzyme reaction. Taken together, these control findings strongly implicate the active enzymes as NADH-linked reductases localized on or within the outer mitochondrial membrane. Final evidence for the electrochemically driven enzymes being part of the NADH-

cytochrome c reductase system was provided by comparing electrochemically derived catalysis rate constants ( $k_{\text{cat}}$ ) to literature rates for maximal substrate turnover ( $V_m$ ). Maximal turnovers measured for the NADH-cytochrome c reductase system in whole rat liver mitochondria are  $V_m = 703 \text{ nmol of TMPD (mg of protein)}^{-1} (\text{min})^{-1}$ ,<sup>21</sup>  $570 \text{ nmol of cytochrome c (mg of protein)}^{-1} (\text{min})^{-1}$ ,<sup>21</sup> and  $620 \text{ nmol of cytochrome c (mg of protein)}^{-1} (\text{min})^{-1}$ .<sup>19</sup> Thus, the maximal turnover rate constants for rat mitochondrial NADH-cytochrome c reductases all fall within a range of  $650 \pm 100 \text{ nmol of acceptor (min)}^{-1} (\text{mg of protein})^{-1}$ . Assuming the same conditions used in the electrochemical assays ( $50 \text{ mM NADH}, 0.5 \text{ mM TMPD}, 35 \text{ mg of protein mL}^{-1}$ ), these average maximal turnover numbers are equivalent to acceptor regeneration rate constants of  $0.8 \pm 0.1 \text{ s}^{-1}$ . Although these are slightly lower than the electrochemically measured values of  $k_{\text{cat}} = 2.0 \pm 0.1 \text{ s}^{-1}$ , the literature kinetic data are basically consistent with the NADH-cytochrome c reductase system being driven electrochemically in the presence of TMPD and NADH.

**SECM Imaging of Glass-Immobilized Mitochondria.** Using the same medium and electrochemical scheme that promoted NADH-cytochrome c reductase catalysis in mitochondrial suspensions described above, we employed the SECM to image the reductase activity of *individual* mitochondria by the feedback mode (Figure 1b). The principles of these experiments and the results were very similar to feedback imaging experiments involving GO. As the microelectrode tip of the SECM was brought near a surface containing immobilized mitochondria, the enzyme acceptor ( $\text{TMPD}^+ = S_1$  in Figure 1b) was constantly produced by applying a positive potential to the tip electrode. If an enzymatically active mitochondrion was under this microelectrode tip and the reductive substrate (NADH) was present in solution in high concentration, the neutral acceptor ( $\text{TMPD}^0 = P_1$  in Figure 1b) was regenerated by the enzyme-catalyzed transfer of electrons from the reductant to the acceptor. This regeneration of  $\text{TMPD}^0$  increased the net current monitored at the tip electrode and indicated an active reductase system on the surface of the mitochondrion. However, if the mitochondrion had an inactive reductase system or the NADH reductant was not present, no regeneration of  $\text{TMPD}^0$  occurred and the mitochondrion merely served to block diffusion from bulk solution to the tip ( $P_1^*$  in Figure 1b), producing the typical SECM insulator negative feedback response. This negative feedback decreased the net current monitored over the mitochondrion compared to  $i_{T,x}$ .

SECM imaging experiments were carried out with glass-immobilized whole mitochondria (see Experimental Section) bathed in an assay electrolyte containing the enzyme-specific reductant  $\beta$ -NADH, as well as the electrochemically oxidizable mediator TMPD ( $50 \text{ mM NADH}, 0.5 \text{ mM TMPD}$ ). Figure 7a shows one of the images obtained with a carbon microelectrode tip ( $a = 4 \mu\text{m}$ ) rastered  $2\text{--}3 \mu\text{m}$  above a mitochondrial-dense region on the glass. In this image, the tip potential was at  $+0.2 \text{ V vs SCE}$  and was scanned at  $10 \mu\text{m s}^{-1}$ . Currents measured at the tip are represented in this image by a gray scale, where the lightest regions correspond to the highest microelectrode currents. The glass surface was easily discriminated in this image, and in all other images, as a uniformly bright field over which individual (ca.  $5\text{--}10\text{-}\mu\text{m}$  diameter) mitochondria were distributed. The image in Figure 7a was particularly interesting because it demonstrated limiting feedback behavior of individual mitochondria. Mitochondria labeled I in Figure 7a appear as dark spots, i.e., current minima, that resulted from purely negative feedback. Such features indicate little or no reductase activity. Although such behavior was only rarely observed with NADH present

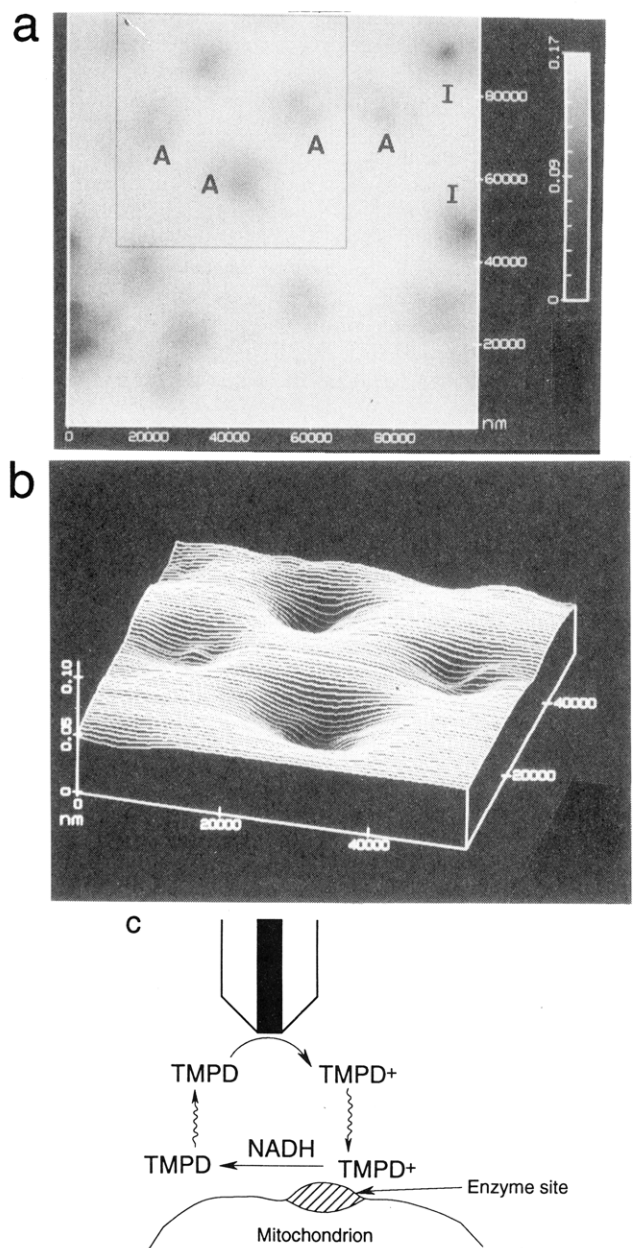


**Figure 7.** SECM image (a,  $100 \times 100 \mu\text{m}$ ) of glass-immobilized mitochondria with boxed region depicted as surface plot (b,  $50 \times 50 \mu\text{m}$ ) for higher contrast. Image was taken with a carbon microelectrode tip ( $a = 4.0 \mu\text{m}$ , RG = 10, rate =  $10 \mu\text{m s}^{-1}$ ) at  $+0.2 \text{ V}$  vs SCE in  $50 \text{ mM}$  phosphate buffer (pH 7.5) containing  $0.1 \text{ M}$  KCl,  $0.25 \text{ M}$  sucrose,  $0.5 \text{ mM}$  TMPD, and  $50 \text{ mM}$  NADH. Lightest image regions depict the greatest normalized tip currents ( $i_i/i_{i,\infty}$ ). Selected enzymatically active mitochondria are labeled A. Inactive mitochondria are labeled I. (c) Schematic representation of SECM conditions for imaging enzyme sites.

in the assay medium (for ca. 1–5% of the mitochondria imaged), in control experiments when NADH was purposely omitted from the electrolyte, all individual mitochondria look like this. Mitochondria labeled A in the figure show increased tip currents (lighter intensities) that were consistent with reductase-promoted regeneration of  $\text{TMPD}^0$ . These features indicated an enzymatically active organelle. A contour image (Figure 7b) of the boxed region in Figure 7a illustrates better these increases in feedback current. Decreased currents at the perimeter of active mitochondria (maximum diameter ca.  $20 \mu\text{m}$ ) were caused by the finite height of these organelles above the glass surface (ca.  $1 \mu\text{m}$ ). This surface relief partially blocked bulk  $\text{TMPD}^0$  from diffusing to the microelectrode tip and decreased the tip current accordingly. Only when the tip was positioned directly above an active mitochondrion

did the reductase catalyze a sufficient regeneration of  $\text{TMPD}^0$  to offset the blocked mass transport.

Although immobilized mitochondria could be imaged successfully with the SECM, a common difficulty experienced during these experiments was the unpredictable loss of mitochondria from the glass surface after even brief exposure to the assay solution. The cause of this spontaneous detachment was unclear, because some immobilized samples remained intact for periods longer than 1 h. Sample immobilization presents significant difficulties in the use of the SECM to image microscopic biological structures.

**Steps for Imaging Enzyme Reactivity with the SECM.** The previous examples illustrate the capability of the SECM to image enzyme reactivity in the feedback mode. However, careful adjustment of the experimental conditions was needed before these experiments could be successfully carried out. One had to address quantitatively (a) whether the enzyme could be sensitively and selectively detected under a particular set of experimental conditions, (b) whether the assay solution and constituents were compatible with fast and reversible electrode reactions, and (c) whether any solution reactions could occur that might compete significantly with the targeted enzyme reaction. Points b and c were addressed using standard electroanalytical techniques and theory. Point a, however, required some knowledge of the enzyme substrate specificity, its limiting redox kinetics, and its concentration within the sample before it could be quantified. Reaction selectivity was not a factor that was directly tested in experiments with the glucose oxidase or NADH–cytochrome  $c$  ( $b_5$ ) reductase systems. However, high reductant specificity was an important parameter in choosing these enzymes for SECM imaging. Sensitivity was of more concern in these experiments. To obtain significant positive feedback to the tip (superimposed on the negative feedback resulting from blockage of diffusion of mediator), the enzyme–mediator reaction had to be sufficiently fast. This was gauged by applying the detection limit criterion (eq 1) previously derived for SECM-induced, zero-order catalysis of two substrate enzymes.<sup>9</sup>

$$k_{\text{cat}} l c_{\text{enz,tot}} \geq 10^{-3} D_R c_R / a \quad (1)$$

To achieve detectable electrocatalytic currents, the combined enzyme-dependent terms for enzyme turnover rate ( $k_{\text{cat}}$ ) and surface concentration ( $l c_{\text{enz,tot}}$ ) had to be greater than combined experimentally controllable factors such as diffusion coefficient for the reduced acceptor ( $D_R$ ), its concentration ( $c_R$ ), and the microelectrode radius ( $a$ ). Although zero-order acceptor turnover at an infinitely planar enzyme surface is assumed in this equation,<sup>9</sup> it still provides a useful guide for assessing the feasibility of local reaction imaging.

Application of the detection criterion to patterned glucose oxidase was simplified by our previous kinetic study of this enzyme system.<sup>9</sup> For the 50% (w/w) hydrogel matrix used to immobilized GO, we could assign to the enzyme term in eq 1 ( $k_{\text{cat}} l c_{\text{enz,tot}}$ ) the previously measured zero-order regeneration rate constant of  $6 \times 10^{-11} \text{ mol cm}^{-2} \text{ s}^{-1}$ . From this value, we selected conditions to make the experimental term ( $10^{-3} D_R c_R / a$ ) sufficiently small to satisfy eq 1. With the carbon microelectrode size limited to  $a = 4 \mu\text{m}$  and with hydroquinone acting as the reduced acceptor ( $D_R = 7.75 \times 10^{-6} \text{ cm}^2 \text{ s}^{-1}$ ), the hydroquinone concentrations necessary for SECM detection of GO were predicted to be  $c_R \leq 0.3 \text{ mM}$ . Accordingly, the hydroquinone concentration was set at  $0.05 \text{ mM}$  for the successful imaging experiment shown in Figure 5.

Experimental conditions for the mitochondrial samples were chosen in a similar way. The enzyme terms for the NADH–cytochrome  $c$  reductase system were estimated from the cyclic voltammetry measurements of  $k_{\text{cat}}$  on suspended mitochondria (described above) and from estimates of enzyme

surface concentration ( $lc_{enz,tot}$ ). Because cytochrome  $b_5$  forms an integral part of the targeted reductase system,<sup>21</sup> its content within the outer mitochondrial membrane was used to estimate the total enzyme surface concentration. Sottocassa et al.<sup>19</sup> reported 0.716 nmol of cytochrome  $b_5$  (mg of outer membrane protein)<sup>-1</sup>, with outer membrane protein making up only 9% of the total protein of whole rat liver mitochondria. The total protein content of a single mitochondrion was estimated to be  $4.6 \times 10^{-9}$  mg,<sup>24</sup> and the total cytochrome  $b_5$  content of the outer membrane of a single mitochondrion was estimated to be  $3.0 \times 10^{-19}$  mol (i.e., about 180 000 molecules). Based on optical photographs (Figure 3) and electron microscopy studies of whole mitochondria,<sup>5</sup> these organelles have an oblate spheroid geometry with a major axis length of 4  $\mu\text{m}$  and minor axis length of 2  $\mu\text{m}$ . These dimensions correspond to an individual mitochondrial surface area of  $2.8 \times 10^{-7} \text{ cm}^2$ .<sup>25</sup> With this information, it was possible to estimate the NADH-cytochrome *c* reductase concentration averaged across the outer membrane of a single mitochondrion as  $1.1 \times 10^{-12} \text{ mol cm}^{-2}$ . Combined with the  $k_{cat}$  value measured electrochemically on whole suspended mitochondria ( $k_{cat} = 2.0 \text{ s}^{-1}$ ), a zero-order regeneration rate constant of  $2.2 \times 10^{-12} \text{ mol cm}^{-2} \text{ s}^{-1}$  was estimated for the reductase system. From this enzyme term and the experimental terms for  $D_R$  (TMPD<sup>0</sup>,  $3.0 \times 10^{-6} \text{ cm}^2 \text{ s}^{-1}$  in the assay electrolyte) and  $a = 4.0 \mu\text{m}$ , the maximum mediator concentration for reductase detection was calculated from eq 1 to be  $c_R \leq 0.3 \text{ mM}$ . Imaging experiments were performed somewhat above this concentration of reduced acceptor (Figure 7, [TMPD] = 0.5 mM) because small tip-surface separation ( $d/a \approx 0.5$ ) were needed to improve lateral image resolution.<sup>7</sup> Without adding the maximum allowed mediator concentration, the primarily negative feedback currents were often too small ( $\leq 50 \text{ pA}$ ) to measure accurately. The direct consequence of operating near the detection limits for the NADH-cytochrome *c* reductase system was the relatively small positive feedback electrocatalytic currents observed in the reductase images (Figure 7).

**Spatial Resolution of Enzyme Reactions with the SECM.** One important feature of the feedback method for detecting and analyzing enzyme surface reactions is its ability to both control and monitor where catalysis actively occurs. However, this arrangement is only possible for localized detection with relatively fast enzyme reactions. For slow enzyme reactions, collection-mode experiments such as those demonstrated with potentiometric<sup>26</sup> and other sensors<sup>27</sup> may be better suited for imaging. The advantage of a passive sensor can be traced to the diffusional nature of the SECM technique. In the amperometric feedback mode (Figure 1b), the reaction site is only active in the immediate presence of the SECM tip and the enzyme must turn over and form its

(24) Total protein content of isolated whole rat liver mitochondria was measured to be 270 mg (g wet weight)<sup>-1</sup>. Deriving a mitochondrial volume of  $1.7 \times 10^{-11} \text{ cm}^3$  from ref 25 ( $a = 4 \mu\text{m}$ ,  $b = 2 \mu\text{m}$ ) and assuming a density near  $1.0 \text{ g cm}^{-3}$ , the protein content of a single mitochondrion was estimated to be  $4.6 \times 10^{-9} \text{ mg}$ .

(25) Surface area of an oblate spheroid (where  $a$  is the radius major axis, and  $b$  is the radius minor axis) is derived as  $2\pi a^2 + b^2 [\ln(1 + \epsilon)/(1 - \epsilon)]/\epsilon$  and volume is derived as  $(4/3)\pi a^2 b$ , where  $\epsilon = (a^2 + b^2)^{1/2}/a$ ; *Formulas, Facts, and Constants*, 2nd ed.; Fischbeck, H. J., Fischbeck, K. H., Eds.; Springer-Verlag: New York, 1987; p 9.

(26) Horrocks, B. R.; Mirkin, M. V.; Pierce, D. T.; Bard, A. J.; Nagy, G.; Toth, K. *Anal. Chem.* 1993, 65, 1213.

(27) Matsue, T.; Uchida, I. In *Chemical Sensor Technology*; Yamazoe, N., Ed.; Elsevier: Amsterdam, 1991; Vol. 3, pp 263–279, and references therein.

product as fast as required to produce a significant feedback contribution to the SECM tip. If the enzyme cannot maintain a high flux of product to the tip compared to the flux of reactant from the bulk solution, which becomes more likely with very small microelectrode tips, the catalysis reaction becomes undetectable by the SECM.

As indicated in eq 1, electrode size is important in the feedback detection of enzyme electrocatalysis. However, spatial resolution of the SECM is also directly governed by the radius of the microelectrode probe.<sup>7</sup> Thus, for the localization of enzyme reaction sites by the feedback mode, the resolution that is obtainable depends upon the kinetics of the catalyzed reaction. A semiquantitative statement of this relationship can be given by a recasting eq 1 in terms of image resolution.

$$\text{enzyme image resolution} \sim a \geq 10^{-3} D_R c_R / (k_{cat} l c_{enz,tot}) \quad (2)$$

For fast enzyme systems that have zero-order turnover rates exceeding  $10^{-12} \text{ mol cm}^{-2} \text{ s}^{-1}$ , SECM image resolution in the feedback mode can be practically reduced to the micrometer and even the submicrometer level. For slower reactions, however, sensitivity constraints need to be considered and image resolution must be sacrificed in favor of adequate signal detection. In cases where high image resolution must be preserved in the face of slow enzyme kinetics, collection-mode SECM would be the reaction imaging technique of choice. However, in collection (e.g., potentiometric<sup>26</sup>) approaches, the enzyme reaction is not activated by the tip and occurs continually at all sites. Thus, experimental conditions must be chosen to establish steady-state concentration profiles near the enzyme sites.

## CONCLUSIONS

This study has demonstrated the ability of the SECM to image the reactivity of redox enzymes down to the micrometer level. A feedback detection scheme was used to observe the localized reaction of glucose oxidase and mitochondrial-bound NADH-cytochrome *c* reductase. This technique relies on rapid chemical communication between the microelectrode probe and the active enzyme to provide sensitivity. Although this feedback method was successful for the two demonstrated systems because of their relatively fast catalytic turnover, slower enzyme systems would be difficult to study by this approach, particularly if high spatial resolution is required. In these cases, collection-mode operation of the SECM could allow more sensitive detection and could offer greater image resolution. A number of collection-mode schemes are potentially available for enzyme studies and other kinds of surface reactions.<sup>26,27</sup>

## ACKNOWLEDGMENT

The authors appreciate helpful discussions with Dr. David Wipf and are grateful to Prof. Daniel Ziegler and his group for providing helpful advice and for carrying out mitochondrial isolations and protein assays. The support of this research by grants from the Robert A. Welch Foundation and the National Science Foundation (CHE 9214480) is gratefully acknowledged.

RECEIVED for review June 9, 1993. Accepted September 28, 1993.\*

\* Abstract published in *Advance ACS Abstracts*, November 1, 1993.